

Sources of primary cosmic rays

S. E. Pyatovsky¹⁾

Lebedev Physical Institute of the Russian Academy of Sciences

May 30th, 2023

In the paper, a comparative primary cosmic rays (PCR) comparative analysis by E_0 and the spectra of variable stars by periods is carried out in order to establish the causes of irregularities in the spectrum of PCR by E_0 . The study was performed using the public database of the KASCADE-Grande experiment and GCVS and ZTF variable star catalogues. It has been suggested that the acceleration of PCR to high and super-high energies occurs not only on the shock waves of supernovae, but also in bursts of giants and super-giants. The relationship between the periods of variable stars and the maximum energy E_0 of the nuclei of PCRs generated by these types of stars is shown. Irregularities in the PCR spectrum by E_0 are associated with the transition from one dominant stars type to another as E_0 increases. The knee in the PCR spectrum at $E_0 = 3 - 5 \text{ PeV}$ is associated with a decrease in the contribution of SRB variability stars and a further increase in the contribution of Mira variable stars to the PCR flux. The bump in the PCR spectrum with a maximum at $E_0 = 80 \text{ PeV}$, established in the KASCADE-Grande experiment, is formed by giant stars and super-giants of the Mira and SRC variability.

Introduction. The reasons for and type of irregularities in the PCR spectrum by E_0 remain the subject of scientific discussions. The issues are discussed of the so-called knees localization in the spectrum, the "sharpness" of knees, at what energies knees are observed in the spectra of light and heavy nuclei in the mass composition of PCR, and others. Attention is drawn to the issues of localization and the source of the bump in the E_0 spectrum of PCR at energy of about 100 PeV .

Analysis of irregularities in the PCR spectrum at $E_0 = 1 - 100 \text{ PeV}$ was carried out, in particular, in [1]. Figure 1 shows the results of the KASCADE-Grande [2], Tunka and Ice-Top experiments on measuring the energy spectrum of PCR. Special attention should be paid to the results of the GAMMA (GAMMA-07) experiments [3] (Armenia, Mount Aragats) and "Hadron" (Tien Shan high-mountain scientific station), 700 g/cm^2 of atmospheric depth, in which at $E_0 \cong 70 - 100 \text{ PeV}$ intensity peak was registered, shown in Figure 1, which significantly exceeds the data of other experiments. The nature of this irregularity has not been established, and other experiments do not report the presence of a similar peak. It is also unusual that this peak was not observed in the exposures of the GAMMA experiment itself (Armenia), but for other time periods, for example, GAMMA-06, -08, etc. However, it is quite possible that this peak is not a methodological error in the processing of experimental data.

It was shown in [1, 4] that the irregularities in the spectrum of PCR by E_0 following the knee at

$E_0 = 3 - 5 \text{ PeV}$ are due to the departure of PCR mass composition nuclei starting with protons. Using the "min-max of EAS age" method [1], based on the sufficiently large statistics of EAS experimental characteristics obtained in particular in the KASCADE-Grande experiment, it was shown that at $E_0 = 2 - 35 \text{ PeV}$, the mass composition of PCR nuclei remains mixed and corresponds to the CNO group. However, the knee in the nuclei spectrum of the PCR mass composition of the heaviest group is localized before the bump observed at $E_0 = 50 - 100 \text{ PeV}$, which indicates that the bump in the spectrum of PCR at $E_0 = 50 - 100 \text{ PeV}$ is formed by other sources of nuclei and with different acceleration features.

1 Experimental data for bump analysis at $E_0 = 50 - 100 \text{ PeV}$. The bump analysis of the PCR spectrum by E_0 was performed using the data of the KASCADE-Grande experiment [2, 4], the database of which contains characteristics of more than 150 million EASs, including EAS global registration time in the range from 846,252,788 to 1,071,878,399 seconds with the count starting from 01/01/1970.

The characteristic of this irregularity (bump) under study is the slope index γ of the PCR spectrum by E_0 . To estimate the change in γ , a range of $E_0 = 20 - 75 \text{ PeV}$ was chosen located after the knee in the group of the heaviest nuclei in the PCR mass composition of and up to the bump maximum at $E_0 = 80 \text{ PeV}$ established by the KASCADE-Grande collaboration and confirmed in the GAMMA and Hadron experiments. The study of the change in γ was performed with a lag of 10 days,

¹⁾mail: vgsep@ya.ru

ORCID: 0000-0003-2565-1670

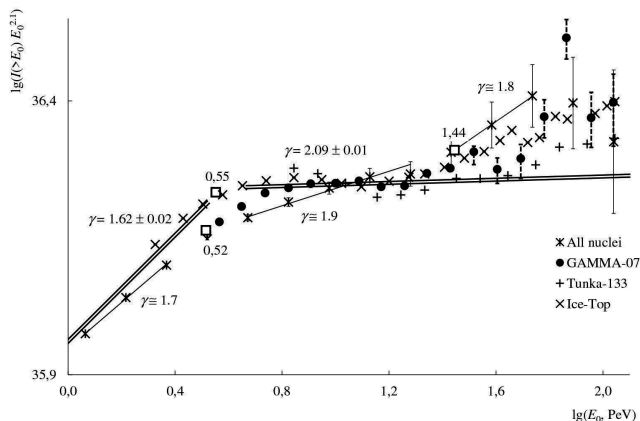


Figure 1. Integral spectra by E_0 obtained in the KASCADE-Grande and GAMMA-07 experiments. The bump maxima in the spectra obtained in the KASCADE-Grande and GAMMA-07 experiments correspond to $E_0 = 50 - 80$ PeV, which is higher than the knee energy of the heaviest nuclei in the PCR mass composition, as shown in [1]. The outlier point (circled) is observed in the PCR spectrum by E_0 confirmed in the GAMMA-07 experiment. The bump with a maximum at $E_0 \cong 80$ PeV was confirmed by the KASCADE-Grande experiment.

which provided statistics for each sample of $\cong 1$ million events.

Examples of spectra for 10-day samples are shown in Figure 2. Figure 2 shows spectra with slope indices γ near the bump at $E_0 = 80$ PeV from the minimum values $\gamma = 1.60 \pm 0.02$ to the maximum values $\gamma = 2.31 \pm 0.04$. The spectra constructed from samples from the KASCADE-Grande experimental data are compared with the data from the GAMMA-07 experiment. Despite the fact that the γ index averaged over the entire observational statistics was obtained with high accuracy, the values of γ for different time intervals differ significantly. This change in γ can be associated either with fluctuations in EAS characteristics, or with the intensity of PCR in the given range E_0 . It also follows from Figure 2 that the outlier event recorded in the GAMMA-07 experiment is not unique and has analogues in the events recorded in the KASCADE-Grande experiment.

Using the database of the KASCADE-Grande experiment, the values of the slope index γ near the bump of the PCR spectrum were obtained in the range of $E_0 = 20 - 75$ PeV for 248 time intervals.

2 Spectral analysis of the change in the γ index. Figure 3 shows the change in the γ index over time. The spectral analysis of the change in γ was per-

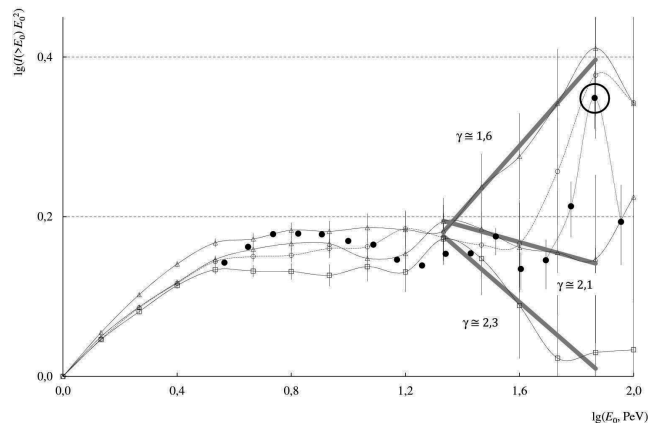


Figure 2. PCR spectrum by E_0 obtained in the GAMMA-07 experiment (black circles, outliers circled) as compared with the data of the KASCADE-Grande experiment for different time intervals (empty markers). Gray lines are regressions in the range of $E_0 = 20 - 75$ PeV (up to the bump maximum at $E_0 = 80$ PeV, established in the KASCADE-Grande experiment).

formed in order to identify possible maxima of the periods of change in γ values. The spectral Fourier transform with the Hamming's window was used for the analysis. It follows from Figure 3 that the change in γ goes beyond the standard deviation, which allows us to assume the presence of regular PCR sources in the range $E_0 = 20 - 100$ PeV.

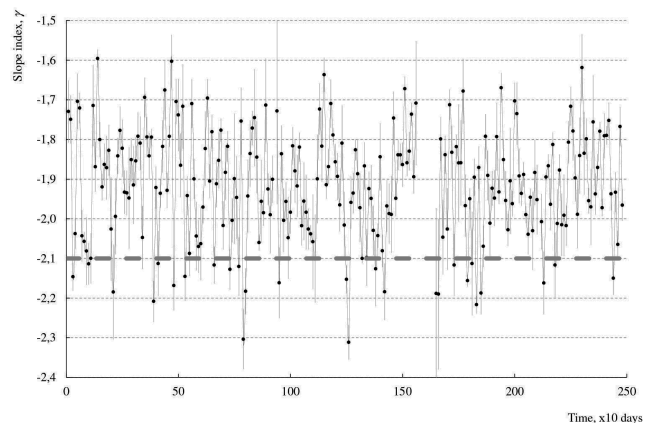


Figure 3. Change in the PCR γ spectrum index by E_0 over time. The horizontal dotted line corresponds to the value of γ in the absence of a bump in the range of $E_0 = 20 - 100$ PeV. The values of γ above this dotted line indicate the presence of a bump with a maximum at $E_0 = 80$ PeV.

The resulting spectral density of the log-period is shown in Figure 4. The analysis made it possible to

identify two maxima in the period of γ change in the interval of 40 – 300 days, equal to 66 and 229 days, corresponding to the maximum spectral density. The width of the spectral density peak characterizes the “locality” of the PCR source: the closer the peak is to the normal distribution, the more likely one PCR source dominates in peak formation. The wider peak is formed by superposition of PCR sources of the same type. In Figure 4, peaks with maxima in periods equal to 66 and 229 days are described by normal distributions with $R_a^2 > 98\%$ (Table 2).

To search for possible PCR sources in the range $E_0 = 20 - 100 \text{ PeV}$, the catalogs of stellar objects "General Catalog of Variable Stars (GCVS)" [5] and "Zwicky Transient Facility Catalog (ZTF)" [6] were considered. More than 60,000 stars of more than 250 types are represented in GCVS with indication of periods, locations and other characteristics. Figure 4 shows that the first harmonic (66 days) corresponds mainly to stars with SR-type variability, while the second harmonic (229 days) is formed mainly by Miras. It also should be noted here that stars that are at the final stages of evolution usually have strong magnetic fields.

The region of transition from semi-regular giants to Miras (Figure 4) is characterized by a local violation of scaling in the PCR spectrum at $E_0 = 3 - 20 \text{ PeV}$ [7]. There should be many local regions similar to those shown in Figure 4 where scaling violation occurs, in the PCR spectrum by E_0 , - scaling violation regions are associated with the transition from one dominant star type to another, and the degree of scaling violations manifestation is determined by energy distributions which are provided by the dominant type of stars of the considered variability.

3 Spectrum of stars by period. The integral spectrum of variable stars depending on the log-period is shown in Figure 5, which shows the periods averaged over the types of variable stars. 252 types of stars have been considered, from white dwarfs of the ZZ Ceti type to super-giants of the recurrent nova type.

Let us assume that the more significant the irregularities in the spectrum by period of PCR sources are, the more significant are the irregularities in the spectrum of PCR by E_0 formed by these sources. The largest irregularities in the spectrum by period are indicated in Figure 5 as the known values of E_0 : the period of 17 days corresponds to $E_0 = 0.1 \text{ PeV}$ (red dwarfs region), 120 days corresponds to $E_0 = 5 \text{ PeV}$ (the bump at $E_0 = 3 - 5 \text{ PeV}$ in the PCR spectrum) and 176 days, - $E_0 = 20 \text{ PeV}$ (beginning of the bump with a maximum at $E_0 = 80 \text{ PeV}$). The acceleration of

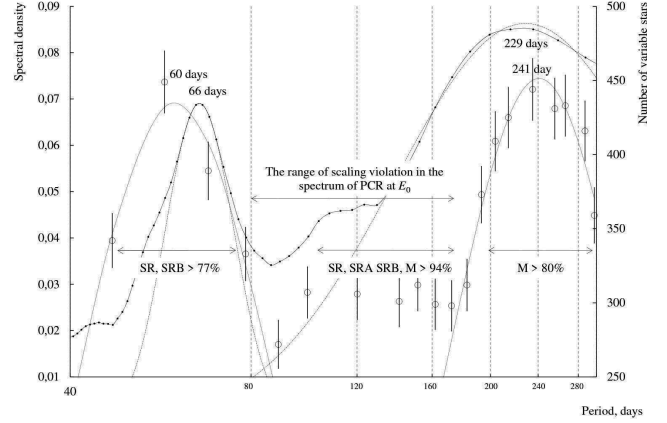


Figure 4. Spectral density of the log-period of the PCR spectrum γ index change by E_0 (solid line, main axis) in comparison with the periods of stars of various types of variability (dashed lines, additional axis): SR - semi-regular red giants and super-giants of intermediate or late spectral classes, SRA and SRB - semi-regular red giants of late M, C and S spectral classes, M - Miras, red giants at the final stages of stellar evolution with emission spectra of late classes.

PCR up to $E_0 = 0.1 \text{ PeV}$ in flares of red dwarfs was established in the works by Yu. I. Stozhkov [8].

Figure 5 shows that PCR sources of low energies $E_0 < 0.1 \text{ PeV}$ are dwarfs localized mainly in the constellations of Sagittarius, Ophiuchus and Centaurus, with medium energies $E_0 = 0.2 - 2 \text{ PeV}$, - sub-giants and giants from the constellations of Sagittarius and Ophiuchi, and high energies $E_0 > 5 \text{ PeV}$, - giants and super-giants from the constellation Sagittarius. It should be noted here that the constellation determines the direction of arrival of PCR of given energies, but not the association with a given group of stars.

From the analysis of the data presented in Figure 5, a regression was obtained that determines the relationship between the average period of a given type of PCR source star and the maximum E_0 :

$$\lg(T, \text{days}) = (0.45 \pm 0.05)\lg(E_0, \text{PeV}) + (1.71 \pm 0.05) \quad (1)$$

Regression (1) is derived from the three hypothesized points shown in Figure 5 (circled). According to formula (1), the lower boundary of the sub-giant region for a period of 23 days is $E_0 = 0.2 \text{ PeV}$, the region of the beginning of the first bump in the PCR spectrum by E_0 is a period of 74 days and $E_0 = 2 - 3 \text{ PeV}$. It is also possible to estimate the maximum PCR energy. According to the GCVS catalog [5], the maximum

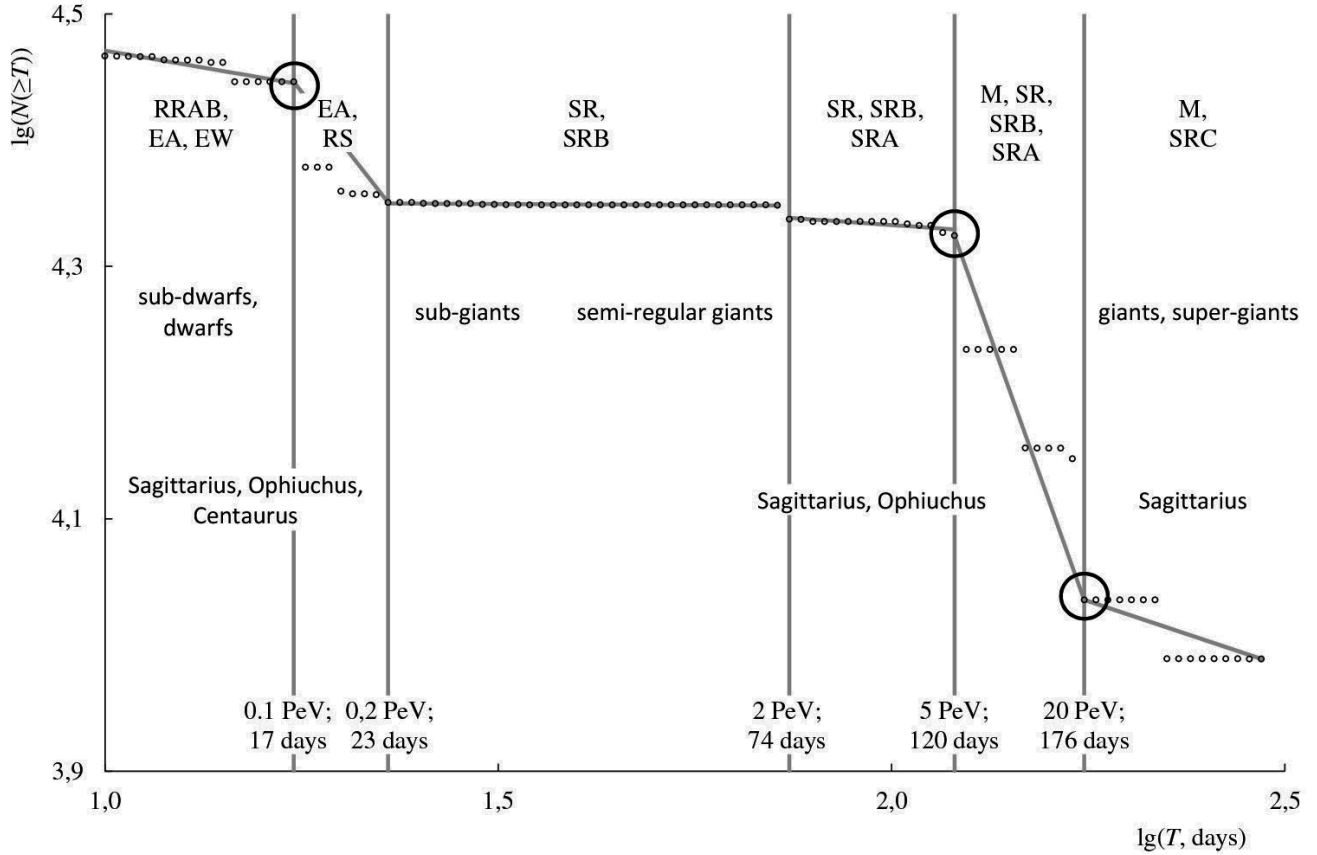


Figure 5. Integral spectrum of variable stars over the log-period (empty circles). The CR acceleration is determined by "the type of variability of a star - the period of a considered star" factor. The dominant types of stars and the constellations where these stars are located are indicated for the indicated intervals by E0 and periods: EA - orange sub-giants of late evolution, EW - contact yellow dwarfs of spectral class F, RS - eruptive yellow-white dwarfs with a secondary component of a magnetically active sub-giant with spectra of Ca-II, H, and K in emission; SRC are semi-regular super-giants of the late M, C, and S spectral classes. Irregularities in the spectrum with assumed values of E_0 are circled.

recorded period is 29,000 days (80 years) for recurrent novae of NR type variability. It follows from formula (1) that the period of 80 years corresponds to the maximum $E_0 \cong 1 - 2 \text{ ZeV}$ registered in CR.

A few more points can be added to the data shown in Figure 5, namely, expert estimates given in Table 1.

The regression built according to the data of Table 1 is similar to (1) within the limits of errors:

$$\lg(T, \text{days}) = (0.41 \pm 0.01)\lg(E_0, \text{PeV}) + (1.71 \pm 0.03), R_a^2 \sim 1 \quad (2)$$

4 Types of variable stars and the PCR spectrum by E_0 . It follows from Figures 4 and 5 that semi-regular giants and Miras make up the main stellar population providing PCR sources at $E_0 = 1 - 100 \text{ PeV}$.

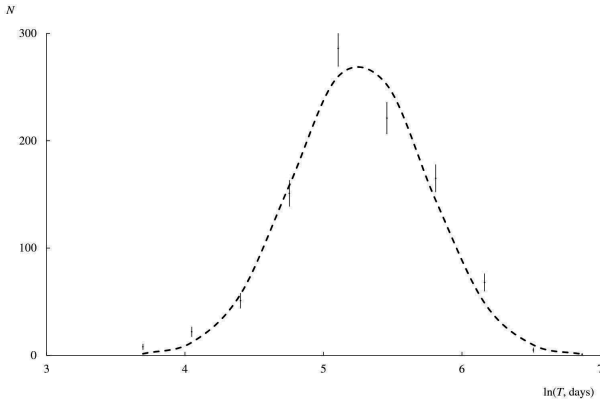
Let us apply the "main array" method and consider the formation by stars of SR, SRA, SRB, and M type variabilities of the PCR spectrum for given E_0 .

The distribution of stars over log-periods corresponds to the normal distribution $N \sim \exp(-\frac{(\ln(T) - \ln(\bar{T}))^2}{2\sigma^2})$ with the parameters given in Table 2. Stars of SRA (193 days), M (280 days) and SRC (372 days) variabilities (Table 2), examples of the distributions of which are given in Figure 6 become closest to the period of 229 days obtained by the Fourier analysis of the change in the PCR spectrum by E_0 γ index (Figure 4).

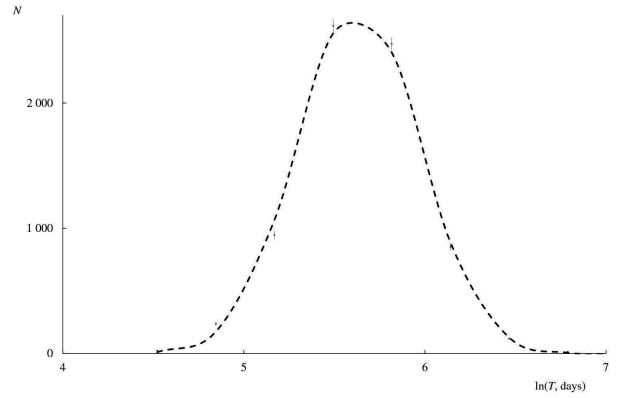
It follows from Figure 6 that the number of Miras is much greater than that of other types of stars with similar periods. It can be assumed that the bump in the PCR spectrum by E_0 around 100 PeV is formed mainly by Miras.

Table 1. Dependence of the log-period of variable stars on the maximum energy E_0 in the PCR spectrum, which these sources provide.

$\lg(E_0, \text{PeV})$	$\lg(T, \text{days})$	Notes
-6.50	-0.93	H spectrum of the Sun
-1.82	1.06	Early break in the spectrum of PCRs (37th RCRC 2022)
-1.00	1.23	Red dwarfs (Yu. I. Stozhkov)
0.48	1.87	Beginning of the first bump in the PCR spectrum
0.70	2.08	The end of the first bump in the PCR spectrum
1.00	2.02	"Vela" local source model (A. D. Erlykin, V. P. Pavluchenko)
1.30	2.25	Beginning of the second bump in the PCR spectrum
6.70	4.46	Maximum registered energy of PCR nuclei



(a)



(b)

Figure 6. Examples of log-period distributions for stars of type variability: (a) SRA (red giants of late spectral classes) and (b) M (red giants at the final stages of stellar evolution).

Table 2. Parameters of log-distributions of stars with SR, SRA, SRB, SRC, and M variabilities.

Star variability	\bar{T} , days	σ	R_a^2
SRB	105	0.75	0.97
SR	124	0.84	0.99
SRA	193	0.49	0.96
M	280	0.34	0.99
SRC	372	0.92	0.90

According to formula (1) and with the parameters of normal distributions given in Table 2, the spectra of stars by E_0 of various types of variability were obtained (Figure 7).

It follows from Figure 7 that, as E_0 increases in the range $E_0 = 1 - 100 \text{ PeV}$, stars at the final stages of stellar evolution start making decisive contribution to PCR, which makes the mass composition of PCR

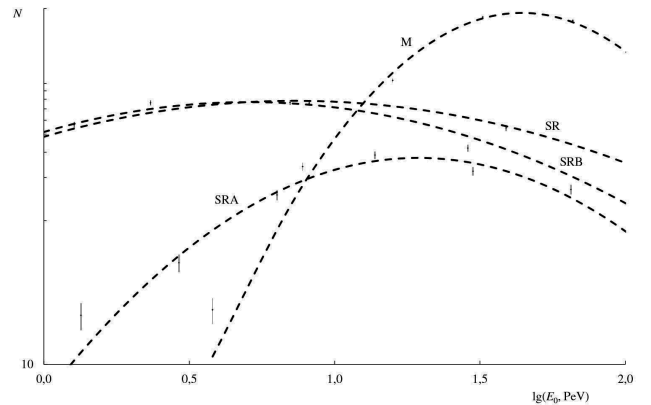


Figure 7. Spectra of stars in log-energy variabilities SR, SRA, SRB, and M of spectral classes M (stars with neutral metals lines), C (carbon stars), and S (zirconium stars).

heavier. However, for each value of E_0 , the PCR mass composition is determined by the dominant type of stars of a given period, which can lead to significant fluctuations in the fraction of different nuclei in the PCR mass composition with change on E_0 .

PCR spectra by E_0 obtained in the GAMMA (Armenia), Tunka-133, Ice-Top and KASCADE-Grande experiments as compared with the spectra of dominant stars of SR, SRA, SRB, SRC and M variabilities obtained from approximations with parameters from Table 2 are shown in Figure 8. The peak of the bump in the PCR spectrum obtained from these approximations is $E_0 \cong 67 \text{ PeV}$.

However, it should be noted that, as follows from Figure 8, the bump should be less pronounced and be at $E_0 < 67 \text{ PeV}$. For example, the average period of SRC variability stars (super-giants) is 372 days, which, according to formula (1), gives the value $\lg(E_0) = 1.91(81 \text{ PeV})$. This value of E_0 corresponds to the results of the KASCADE-Grande experiment. At the same time, the average period of Miras is 280 days, or $\lg(E_0) = 1.64(44 \text{ PeV})$. Because since the number of observed Miras is an order of magnitude greater than that of stars with SRC variability, the localization of the bump maximum according to the KASCADE-Grande experiment at $E_0 = 80 \text{ PeV}$ may be overestimated. It can also be assumed that the bump is formed both by Miras and by SRC super-giant stars.

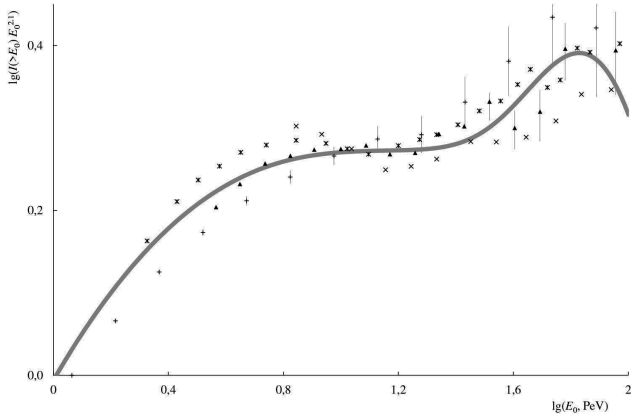


Figure 8. Comparison of PCR spectra by E_0 obtained in the GAMMA (Armenia), Tunka-133, Ice-Top, and KASCADE-Grande experiments with the distribution of SR, SRA, SRB, SRC, and M type variability stars (gray curve).

The types of dominant stars for different E_0 are listed in Table 3. With the increase in the mass of a star (system of stars) the period of the star and the maximum energy E_0 of PCR nuclei, provided by the

acceleration mechanism in flares of this type of star increase.

Figure 9 compares the PCR spectra by E_0 obtained in a number of experiments with the spectrum of variable stars. CR acceleration to ultra-high energies occurs in explosive and nova-like stars, for example, in recurrent novae, in which the maximum period has been registered, providing the maximum $E_0 \sim 1 - 2 \text{ ZeV}$. In the range $E_0 = 200 \text{ PeV} - 3.5 \text{ EeV}$, no stars of variable types have been registered (see Figure 9): ZAND type of variability corresponds to the average period $T = 553$ days, or according to formula (1) $E_0 = 200 \text{ PeV}$, followed by stars of N variability with $T = 2000$ days, or $E_0 = 3.5 \text{ EeV}$.

An example of a binary star system where acceleration to ultra-high energies occurs can be an EA+SRC variability star with a recorded period of 7,430 days (20 years), which should provide a bump in the PCR spectrum at $E_0 = 60 \text{ EeV}$ or $\lg(E_0, \text{PeV}) = 4.80$. It can be a μ Cepheus type star (Herschel's garnet, a red super-giant at the last stage of stellar evolution with a He-C cycle) and an Algol β Perseus type star.

An example of a triple star system where acceleration to ultra-high energies occurs can be a system of UGSU+E+ZZ variability stars with a recorded period of 11,900 days (33 years), which should provide a bump in the PCR spectrum at $E_0 = 180 \text{ EeV}$ or $\lg(E_0, \text{PeV}) = 5.26$. This may be a system of dwarf stars of the SU Ursa Major type (an eruptive dwarf) with super-maximal flares with amplitude of up to 2^m . If this source is considered the only one providing the PCR flux at $E_0 = 180 \text{ EeV}$, then the changes in the PCR flux at a given E_0 over 33 years should be significant, from the maximum to complete decay, which is observed in experiments.

Summarizing the results obtained in this study, let us once again consider the characteristics of variable stars from the GCVS catalog [5]. Let us sort the stars according to the increasing period and construct a double dependence of the log-period and E_0 on the types of eclipsing variable stars shown in Figure 10. This spectrum is characterized by three main regions of irregularities with respect to linear dependence: starting from the RS variability stars, the so-called early knee in the PCR spectrum by E_0 ; starting from SRD type stars (giants and super-giants of spectral classes F, G, or K), there is a knee at $E_0 = 3 - 5 \text{ PeV}$; starting with Miras, - the so-called bump at E_0 about 100 PeV . It should also be noted that, as follows from Figure 10, after the steepening of the PCR spectrum by E_0 after the knee at $3 - 5 \text{ PeV}$, the γ index of the PCR spectrum

Table 3. Types of dominant stars for different E_0 (EA are Algol sub-giants of late evolution, BY are draconian dwarfs (for example, the Sun [9]) of the Ke and Me spectral classes, RS are eruptive stars (a dwarf with a magnetically active sub-giant as secondary component) with Ca-II, H, and K spectra in emission).

Energy, $\lg(E_0, \text{PeV})$	Star period, days	Star type	
< 0.1	< 17	Sub-dwarfs, dwarfs	EA, BY, RS
$0.2 - 2$	$23 - 74$	Semi-regular giants	SR, SRB
> 20	> 176	Giants, super-giants	SR, SRB, SRC, M
$> 10^6$	$> 29,000$	Recurrent novae	NR

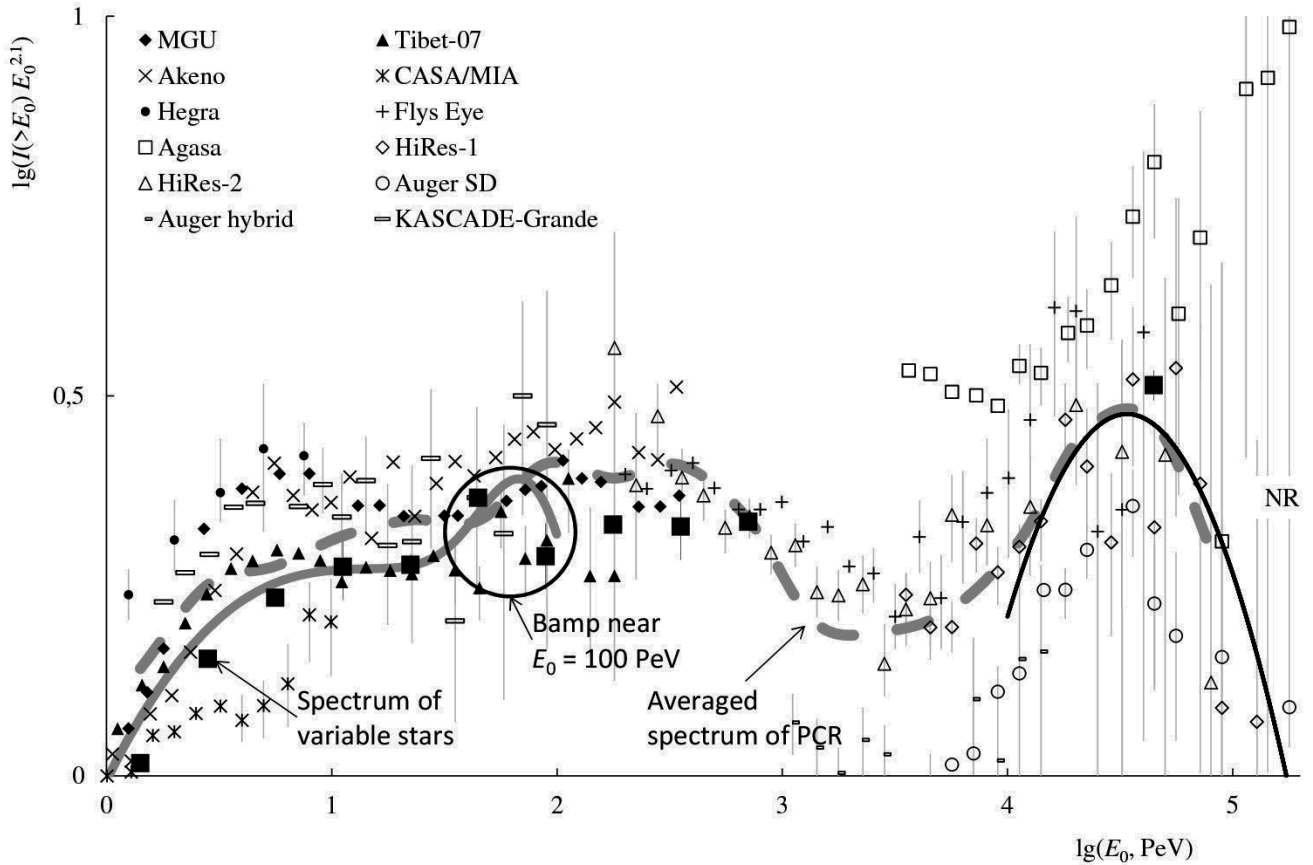


Figure 9. Comparison of the PCR spectra for $E_0 > 1 \text{ PeV}$ obtained in a number of experiments [10–20] with the spectrum of variable stars. A bump near $E_0 = 100 \text{ PeV}$ is provided by the stars of the Miras and SRC variabilities. In the range $E_0 = 200 \text{ PeV} - 3.5 \text{ EeV}$ ($\lg(E_0, \text{PeV}) = 2.3 - 3.5$), there are no stars with the corresponding periods (not registered), which determines the minimum in the PCR spectrum by E_0 in this range.

by E_0 decreases again and becomes approximately the same as it was before the knee.

Conclusions. The relationship between the E_0 spectrum of PCR and the period spectrum of variable stars is shown. It is shown that the bump in the PCR spectrum at $E_0 = 3 - 5 \text{ PeV}$ is explained by the change in the type of source stars in this range of E_0 . The factor of PCR acceleration to high and ultra-high energies not only on supernova shock waves, but also in flares of

giant and super-giant stars is responsible for the shape of the PCR spectrum by E_0 .

1. PCR sources are variable stars of various types, which are at different stages of evolution, from sub-dwarfs to super-giants.
2. CR acceleration to high and super-high energies occurs not only on the shock waves of supernovae, but also in flares of giants and super-giants.

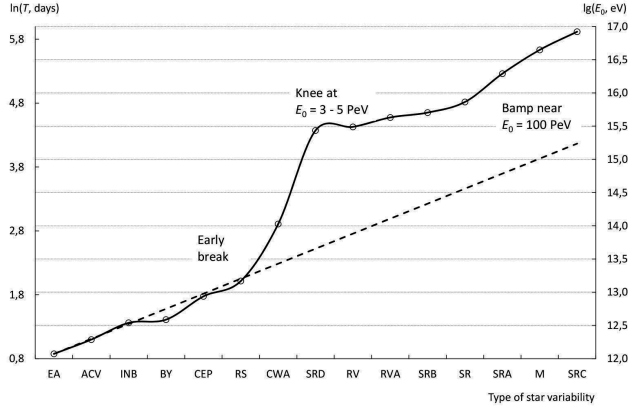


Figure 10. Dependence of stellar periods and energy E_0 on the types of eclipsing variable stars.

3. There is a direct relationship between the average period for a star of a given type of variability and the maximum PCR energy E_0 provided by the acceleration mechanisms on these stars.
 4. A star of each type determines the E_0 PCR range with its flares. Each E_0 range corresponds to the PCR mass composition, which is determined by the type of the source star and which can change significantly with E_0 .
 5. The bump in the PCR spectrum by E_0 about 100 PeV is formed by giants and super-giants of M and SRC variability of late spectral classes. Other types of stars are responsible for other irregularities in the PCR spectrum by E_0 .
 6. The maximum energy E_0 of PCR is determined by recurrent novae and amounts to 1 – 2 ZeV. It is also possible that there are longer-period types of stars that provide higher values of E_0 .
-
1. Erlykin A. D., Puchkov V. S., Pyatovsky S. E. Change in the mass composition of primary cosmic radiation at energies in the range of $E_0 = 1 - 100$ PeV according to data of the KASCADE-Grande experiment//Physics of Atomic Nuclei. - 2021. - Vol. 84. - No 3. - p. 279-286. - DOI: 10.1134/S1063778821030170
 2. T. Antoni, W. D. Apel, F. Badea, K. Bekk, A. Bercuci, H. Blumer, H. Bozdog, I. M. Brancus, C. Buttner, A. Chilingarian, K. Daumiller, P. Doll, J. Engler, F. Febler, H. J. Gils, R. Glasstetter, et al., Nucl. Instrum. Methods Phys. Res., Sect. A 513, 490 (2003). - DOI: 10.1016/S0168-9002(03)02076-X
 3. A. P. Garyaka, R. M. Martirosov, S. V. Ter-Antonyan, A. D. Erlykin, N. M. Nikolskaya, Y. A. Gallant, L. W. Jones, and J. Procureur, J. Phys. G: Nucl. Part. Phys. 35, 115201 (2008); arXiv: 0808.1421v1 [astro-ph]. - DOI: 10.1088/0954-3899/35/11/115201
 4. Apel W., Arteaga J. C., et al. The KASCADE-Grande experiment//KASCADE-Grande Collaborations, Nucl. Instrum. Methods Phys. Res. A 620 (2-3) (2010), pp. 202-216. - DOI: 10.1016/j.nima.2010.03.147
 5. General Catalogue of Variable Stars//The Sternberg Astronomical Institute, The Institute of Astronomy of Russian Academy of Sciences. URL: <http://www.sai.msu.su/gcvs/>
 6. C. Xiaodian, W. Shu, D. Licai, et al. The Zwicky Transient Facility Catalog of Periodic Variable Stars//The Astrophysical Journal Supplement Series, 249:18 (21pp), 2020 July. DOI - 10.3847/1538-4365/ab9cae
 7. S. B. Shaulov, V. A. Ryabov, A. L. Schepetov, S. E. Pyatovsky, et al. Strange quark matter and the astrophysical nature of anomalous effects in cosmic rays at energies of 1 – 100 PeV//Letters to the Journal of Experimental and Theoretical Physics. 2022. 1-2(7). 116. c. 3-12. DOI - 10.31857/S1234567822130018
 8. V. G. Sinitsyna, V. Yu. Sinitsyna, Yu. I. Stozhkov. Red dwarf stars as a new source type of galactic cosmic rays//Astronomische Nachrichten. 2021. 342. 1-2. pp. 342-346. DOI - 10.1002/asna.202113931
 9. I. Yu. Alekseev. Statistics of BY Draconis Variables//Astron. Rep. 44, 696-700 (2000). DOI - 10.1134/1.1312966
 10. De Mitri I. on behalf of the ARGO-YBJ Collaboration. Measurement of the cosmic ray all-particle and light-component energy spectra with the ARGO-YBJ experiment//ISVHECRI 2014. - 18th International Symposium on Very High Energy Cosmic Ray Interactions, EPJ Web of Conferences. - 2015. - 99. p. 08003. - DOI: 10.1051/epjconf/20159908003
 11. Apel W. D., Arteaga-Velazquez J. C., et al. KASCADE-Grande measurements of energy spectra for elemental groups of cosmic rays//Astropart. Phys. - 2013. - 47. - pp.54-66. - DOI: 10.1016/j.astropartphys.2013.06.004
 12. Apel W. D., Arteaga J. C., et al. Energy spectra of elemental groups of cosmic rays: Update on the KASCADE unfolding analysis//Astropart. Phys. 31 (2009), 2, pp. 86-91. - DOI: 10.1016/j.astropartphys.2008.11.008
 13. Schoo S., Kang D., et al. - KASCADE-Grande Collaboration. A new analysis of the combined data from both KASCADE and KASCADE-Grande//Proceedings of the 35th International Cosmic Ray Conference. - 2017. - PoS(ICRC2017). - 339
 14. Kampert K.-H., Unger M. Measurements of the cosmic ray composition with air shower experiments//Astropart. Phys. - 2012. - 35. - pp.660-678. - DOI: 10.1016/j.astropartphys.2012.02.004
 15. Budnev N., Astapov I., et al. The TAIGA experiment - a hybrid detector for very high energy gamma-ray

-
- astronomy and cosmic ray physics in the Tunka valley//Proceedings of the 35th International Cosmic Ray Conference. - 2017. - PoS(ICRC2017). - 768
16. Fedorov O., Bezyazeev P. A., et al. - Tunka-Rex Collaboration. Detector efficiency and exposure of Tunka-Rex for cosmic-ray air showers//Proceedings of the 35th International Cosmic Ray Conference. - 2017. - PoS(ICRC2017). - 387
 17. Sveshnikova L., Astapov I., et al. Search for gamma-ray emission above 50 TeV from Crab Nebula with the TAIGA detector//Proceedings of the 35th International Cosmic Ray Conference. - 2017. - PoS(ICRC2017). - 677
 18. Porelli A., Wischnewski R., et al. TAIGA-HiSCORE detection of the CATS-LIDAR on the ISS as fast moving point source//Proceedings of the 35th International Cosmic Ray Conference. - 2017. - PoS(ICRC2017). - 754
 19. Postnikov E., Astapov I., et al. Commissioning the joint operation of the wide angle timing HiSCORE Cherenkov array with the first IACT of the TAIGA experiment//Proceedings of the 35th International Cosmic Ray Conference. - 2017. - PoS(ICRC2017). - 756
 20. Kopper C. - IceCube Collaboration. Observation of Astrophysical Neutrinos in Six Years of IceCube Data//Proceedings of the 35th International Cosmic Ray Conference. - 2017. - PoS(ICRC2017). - 981